Available online at www.sciencedirect.com
SCIENCE DIRECT®
Journal of Sound and Vibration 278 (2004) 527–537
JOURNAL OF SOUND AND VIBRATION
www.elsevier.com/locate/jsvi

Leak noise propagation and attenuation in submerged plastic water pipes

J.M. Muggleton*, M.J. Brennan

Institute of Sound and Vibration Research, Southampton University, Highfield, Southampton SO17 1BJ, UK

Received 12 June 2003; accepted 9 October 2003

Abstract

Detection of water leaks in buried distribution pipes using acoustic methods is common practice in many countries. Correlation techniques are widely used in leak detection, and these have been extremely effective when attempting to locate leaks in metal pipes. However, a number of difficulties have been highlighted when trying to determine the position of leaks in plastic pipes. Of particular interest here is what happens to the leak noise when the pipe passes through an expanse of water, such as across a river or lake.

In this paper, the low-frequency acoustic propagation and attenuation characteristics of a submerged plastic water pipe are investigated experimentally in the laboratory, supported by predictions from a theoretical model. It is found that, whilst the signal attenuation for a submerged pipe is increased relative to that for a similar in-vacuo pipe, energy does not, in fact, radiate into the water; furthermore, the attenuation is small compared with that for a pipe buried in soil.

1. Introduction

Detection of water leaks in buried distribution pipes using acoustic methods is common practice in many countries [1,2]. Correlation techniques are generally used to locate the leaks, and although these techniques have been successful for many years when used with metal pipes, they remain problematic when used with plastic pipes [3], with a number of difficulties being highlighted. Of particular interest here is what happens to the leak noise when the pipe passes through an expanse of water, such as across a river or lake. Leak detection personnel frequently report that a leak signal that is clearly detectable prior to the pipe passing through the water is no

*Corresponding author. Tel.: +44-23-8059-2936; fax: +44-23-8059-3190.
E-mail address: jm9@soton.ac.uk (J.M. Muggleton).

0022-460X/$ - see front matter
doi:10.1016/j.jsv.2003.10.052

longer detectable afterwards, although, to the authors' knowledge, the exact circumstances have never been clearly documented.

A low-frequency theoretical model of a buried fluid-filled pipe to predict both wavespeed and attenuation was developed by Muggleton et al. [4], and validated experimentally for the case of an in-vacuo pipe, and a pipe buried in soil [5]. Leak noise is generally considered to be concentrated at frequencies less than 100 Hz [2] so it is this low-frequency regime which is of most interest.

Here, the particular case of a submerged plastic water pipe is investigated, the laboratory measurements being supported by predictions from the theoretical model.

2. Theory

At frequencies much less than the pipe ring frequency, four wave types are responsible for most of the energy transfer in a fluid-filled elastic pipe [6,7]: three axisymmetric waves, n=0, and the n=1 wave, related to beam bending. Of the n=0 waves, the first, termed s=1, is a predominantly fluid-borne wave; the second wave, s=2, is predominantly a compressional wave in the shell; the third wave, s=0, is a torsional wave uncoupled from the fluid. Acoustic energy in buried water pipes generated by a leak propagates at relatively low frequencies, generally less than 200 Hz, and so it is the low-frequency dynamics of the system, well below the ring frequency of the pipe, that is of interest. Furthermore, it is found that it is the $s=1$ fluid-dominated wave which predominates.

The pipe equations for n=0 axisymmetric wave motion for a fluid-filled pipe, both in-vacuo and surrounded by an infinite elastic medium have been derived previously [4,6], and expressions for the wavenumbers for the $s=1$ and 2 waves have been found. The $s=1$ wave is the focus of attention here, and for clarity, the results for this wave, for an in-vacuo pipe and a submerged pipe are reproduced.

2.1. The fluid-borne s=1 wave

For an in-vacuo pipe at low frequencies, the $s=1$ wavenumber, k_1, is equal to the free field wavenumber, k_f, modified by a term containing the ratio of the fluid stiffness to the radial pipe wall stiffness:

$$k_1^2 = k_f^2\left(1 + \frac{2B_f/a}{Eh/a^2}\right), \tag{1}$$

where B_f is the bulk modulus of the contained fluid; a and h are the radius and thickness of the shell wall, respectively ($h \ll a$); and E is the Young's modulus of the shell material, which may be complex if the material is lossy ($E \to E(1+\mathrm{i}\eta)$ where η is the material loss factor). This is the familiar non-dispersive Korteweg equation [8].

The equation shows that, for a rigid walled pipe, the $s=1$ wavenumber is equal to the free field wavenumber. As the flexibility of the pipe wall increases, the $s=1$ wavenumber increases, and the wavespeed of the $s=1$ wave decreases correspondingly. The effect of a lossy pipe wall material (represented by a complex Young's modulus) is to introduce a small and negative imaginary component into the wavenumber, indicating that the $s=1$ wave decays as it propagates.

At slightly higher frequencies (but still below the pipe ring frequency), inertial terms must be taken into account, and the wavenumber k_1 becomes [4,6]

$$k_1^2 = k_f^2\left(1 + \frac{2B_f/a}{Eh/a^2 - \omega^2\rho h}\right) = k_f^2\left(1 + \frac{z_{fluid}}{z_{pipe}}\right) \tag{2}$$

where the fluid and pipe impedances are given by $z_{fluid} = -2\mathrm{i}B_f/(a\omega), z_{pipe} = \mathrm{i}\left(\rho h\omega - Eh/(a^2\omega)\right)$; ω is the angular frequency and ρ is the density of the shell material.

When the pipe is immersed in a surrounding medium, the $s = 1$ wavenumber becomes a function of the radiation impedance, z_{rad}, as well as the fluid and pipe wall impedances [4]:

$$k_1^2 = k_f^2\left(1 + \frac{z_{fluid}}{z_{pipe} + z_{rad}}\right), \tag{3}$$

where

$$z_{rad} = \sum_m \frac{-\mathrm{i}\rho_m c_m k_m}{k_{m1}^r}\frac{\mathrm{H}_0(k_{m1}^r a)}{\mathrm{H}_0'(k_{m1}^r a)}. \tag{4}$$

ρ_m, c_m, and k_m are the density, wavespeed and wavenumber respectively of each wavetype present in the surrounding medium, and the summation is performed over all wavetypes present. For the case of a surrounding fluid, only one wavetype will be present. k_{m1}^r, is the radial component of the wavenumber in the fluid, given by

$$(k_{m1}^r)^2 = k_m^2 - k_1^2. \tag{5}$$

H_0 is a Hankel function of the second kind, representing outgoing waves when the $\mathrm{e}^{\mathrm{i}\omega t}$ time dependence is adopted, and the prime denotes differentiation with respect to the argument. It is assumed that the surrounding medium is of infinite extent, so that no incoming waves are present.

When the argument of the Hankel function is purely (or predominantly) real, it is found that the radiation impedance is complex, with positive real and imaginary components [9,10]. Conversely, when the argument of the Hankel function is purely (or predominantly) imaginary, the resulting radiation impedance is purely (or predominantly) imaginary and positive [9,10]. Because the imaginary part of the radiation impedance is always positive, the surrounding fluid effectively mass loads the pipe. When the real part of the impedance (the radiation resistance) is positive, energy radiates into the fluid.

Returning to Eq. (5), when the pipe is surrounded by water, $k_m \ll k_1$, so the radial wavenumber k_{m1}^r will be predominantly imaginary, resulting in a predominantly imaginary radiation impedance. This is discussed in more depth in the following section, when the experimental data are examined.

3. Wavenumber measurements on the submerged pipe

3.1. Experimental set-up and procedure

The experimental arrangement is shown in Figs. 1a–c. It consisted of a water-filled MDPE pipe, approximately 2 m in length, secured vertically, with the lower end sealed (Fig. 1a). The water column was excited at the upper end by an electrodynamic shaker attached to a light, rigid piston

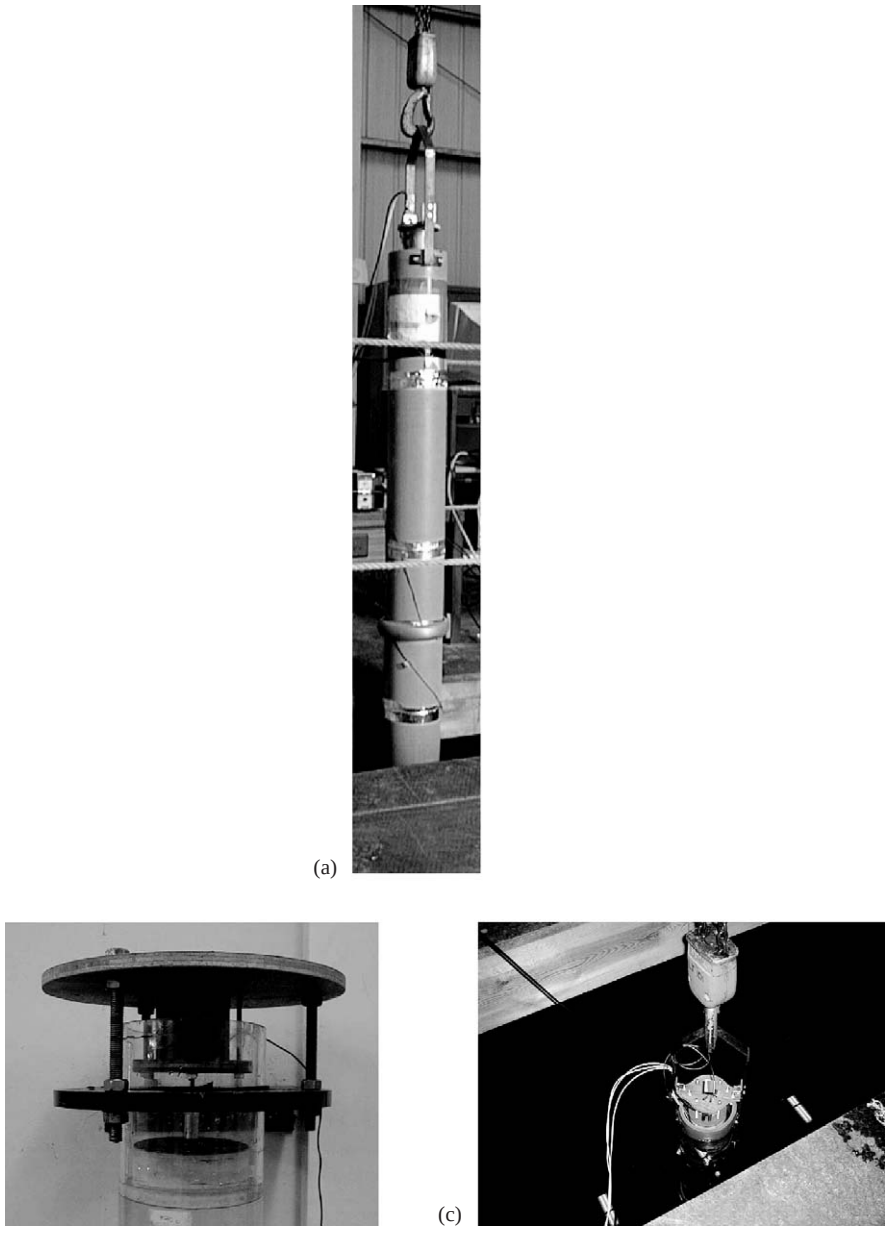

Fig. 1. (a) MDPE pipe suspended above the tank. (b) Close-up of exciter and piston (shown here on perspex pipe for clarity). (c) Pipe rig suspended in water tank.

(Fig. 1b). The centre section of the pipe was instrumented with three hydrophones suspended along the centreline inside the pipe, spaced 0.5 m apart. The pipe was then suspended in a large water tank (8 m × 8 m × 5 m deep), filled almost up to the rim (Fig. 1c). The piston was excited with a stepped sine input from 30 Hz to 1 kHz at 1 Hz intervals, and the signals from the

transducers acquired into a digital analyzer. The experiment was then repeated with the pipe suspended above the water, in air (to simulate the in-vacuo case), for comparison.

3.2. Experimental results and comparison with theory

The experimentally determined wavenumbers for both the in-air and in-water cases were calculated using a three transducer method described previously [5], as the pipe was not terminated anechoically, and this method allows for unknown boundary conditions at either end of the pipe. The predicted wavenumber was calculated using Eq. (1) for the immersed pipe, and Eq. (5) for the in-air pipe, along with previously measured values of the pipe material and geometrical properties (shown in Table 1). The density and wavespeed of water were assumed to be 1000 kg/m^3 and 1500 m/s respectively. The real and the imaginary components of the measured and predicted wavenumbers are shown in Figs. 2a–c. The imaginary part is expressed as wave attenuation in dB/m where

$$Loss\,(\mathrm{dB/m}) = \frac{20\,\mathrm{Im}\{k\}}{\ln(10)}.$$

Fig. 2a shows that there is good agreement between the measured and predicted values for the real part of the wavenumber, for both the in-air and in-water measurements. As discussed previously [5,6], the effect of the pipe wall flexibility is to significantly reduce the wavespeed of the 'fluid-borne' wave from the free-field case (for the in-air pipe, to around 300 m/s at 500 Hz compared with 1500 m/s). The presence of the surrounding water effectively mass loads the pipe [4,11] and so reduces the wavespeed yet further. This trend is seen clearly in both the measurements and the predictions, the wavespeed at 500 Hz reducing to around 270 m/s. The slight unevenness in the measured curves is thought to be associated with small errors in decomposing the outgoing and reflected waves in the pipe, as well as in the phase unwrapping [5].

Figs. 2b and c (plotted separately for clarity) show that the agreement between the measured and predicted data for the imaginary part of the wavenumber is less than for the real part. The mean values for the measured data show good agreement but the deviations from the mean are larger. Again, the deviations from the mean in the measured curves are thought to be associated with wave decomposition and phase unwrapping [5]. For the in-air case, the attenuation is largely due to losses within the pipe wall, as it inflates and deflates in response to the internal fluid pressure. The predicted attenuation is greater for the in-water case, and this is borne out by the measurements. This might suggest that, even though the wavespeed in the water is high compared with the wavespeed of the 'fluid-borne' wave, the 'fluid-borne' wave radiates into the surrounding

Table 1
Geometrical and material properties of MDPE pipe

Mean radius (m)	84.5×10^{-3}
Wall thickness (m)	11×10^{-3}
Density (kg/m^3)	900
Young's modulus (GN/m^2)	1.6
Loss factor	0.06

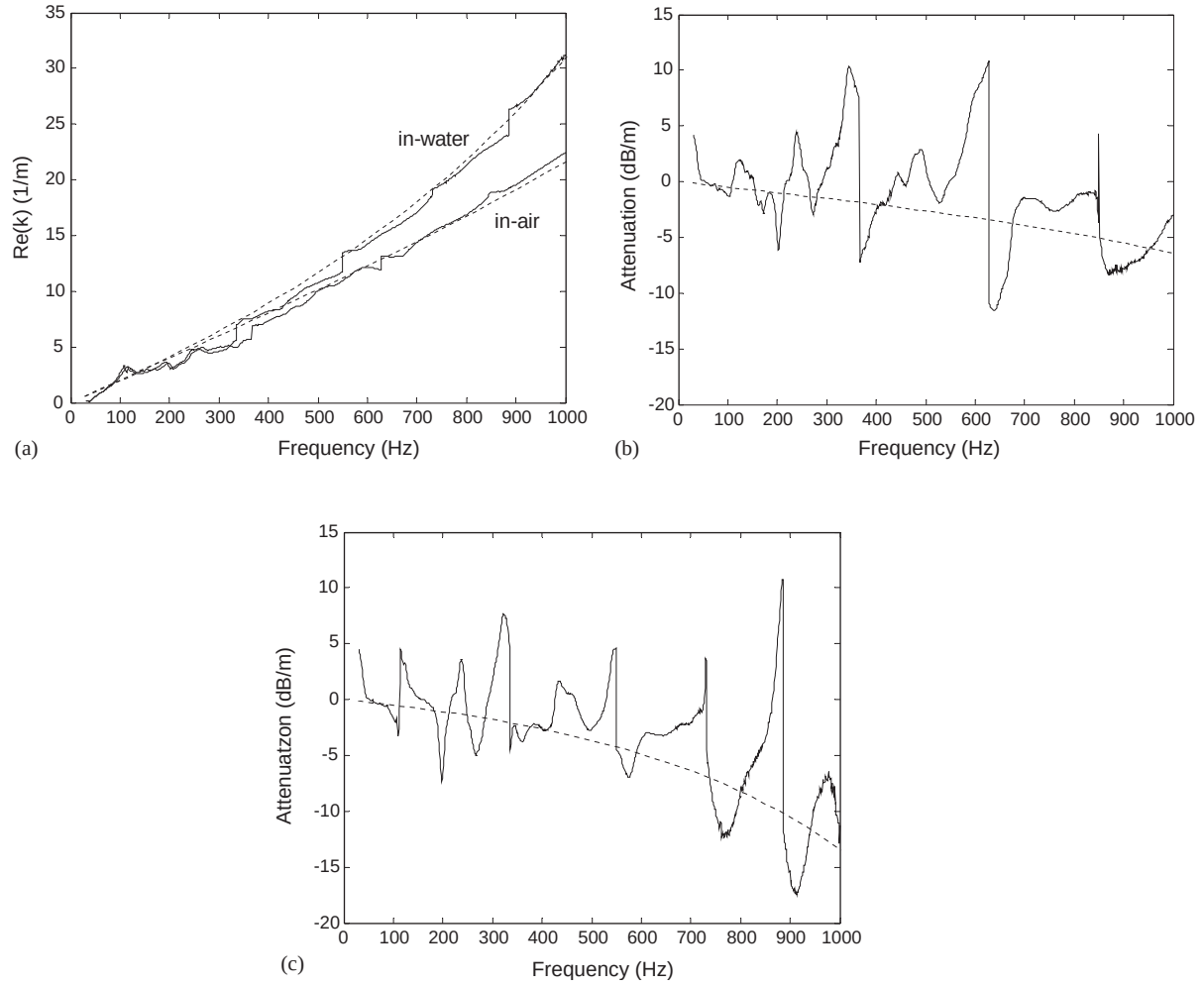

Fig. 2. Wavenumber for the axisymmetric 'fluid-borne' wave: (a) real part; (b) imaginary part (in-air); (c) imaginary part (in-water) - -, predicted; —, measured.

medium. However, examination of the predicted component impedances in Eq. (4), shown in Fig. 3, reveals that this is not, in fact, the case. The real part of the radiation impedance (radiation resistance) is extremely small compared with the pipe wall loss term (and in fact negative[1]), and the cause of the increase in wave attenuation is the slowing down of the wave and concomitant decrease in wavelength, rendering the pipe wall loss mechanism more effective.

[1] The negative radiation resistance, at first sight unphysical is, in fact, consistent with the modelling assumptions, although it reveals a slight anomaly in the model. The model, which is essentially modal, requires that the wavenumber component in the direction along the pipe is the same in the pipe and the surrounding medium at all radii. For the case of a lossy pipe wall material the wave decays along the pipe; it must also then decay in the surrounding fluid in the pipe direction. However if (as in this case) the surrounding fluid is non-lossy, the only way the wave here can decay is if energy is transferred from the fluid to the pipe. This results in the negative radiation resistance seen here. This slightly disconcerting effect is the subject of current investigation.

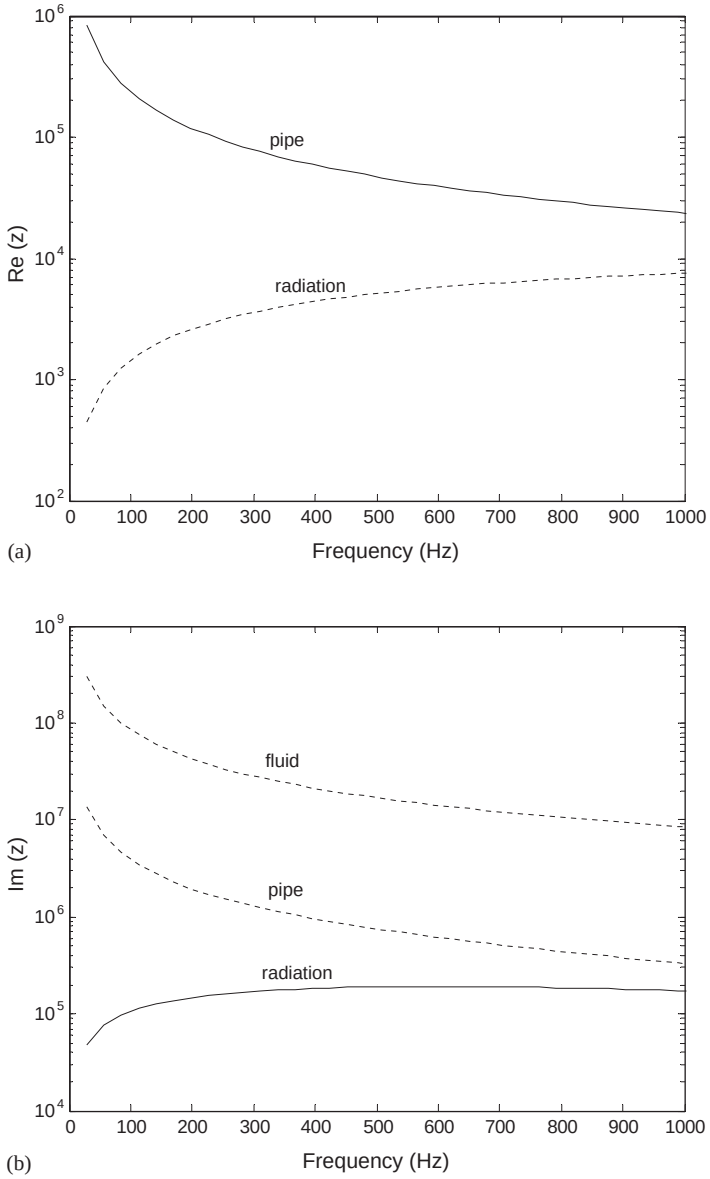

Fig. 3. Component impedances for submerged pipe (predicted): (a) real part; (b) imaginary part. (dotted lines indicate negative values).

For comparison, results obtained previously [5] for a similar MDPE pipe buried in sandy soil are shown in Figs. 4a and b. The soil parameters used in the predictions are shown in Table 2. The low wavespeeds in the soil indicate that, in this case, the radial wavenumbers (Eq. (5)) for both wavetypes will be predominantly real, resulting in a radiation impedance which has both positive-real and positive-imaginary components. Under these circumstances energy will be radiated from the pipe into the soil. This is evident in the figures which show that, even though the wavespeed is

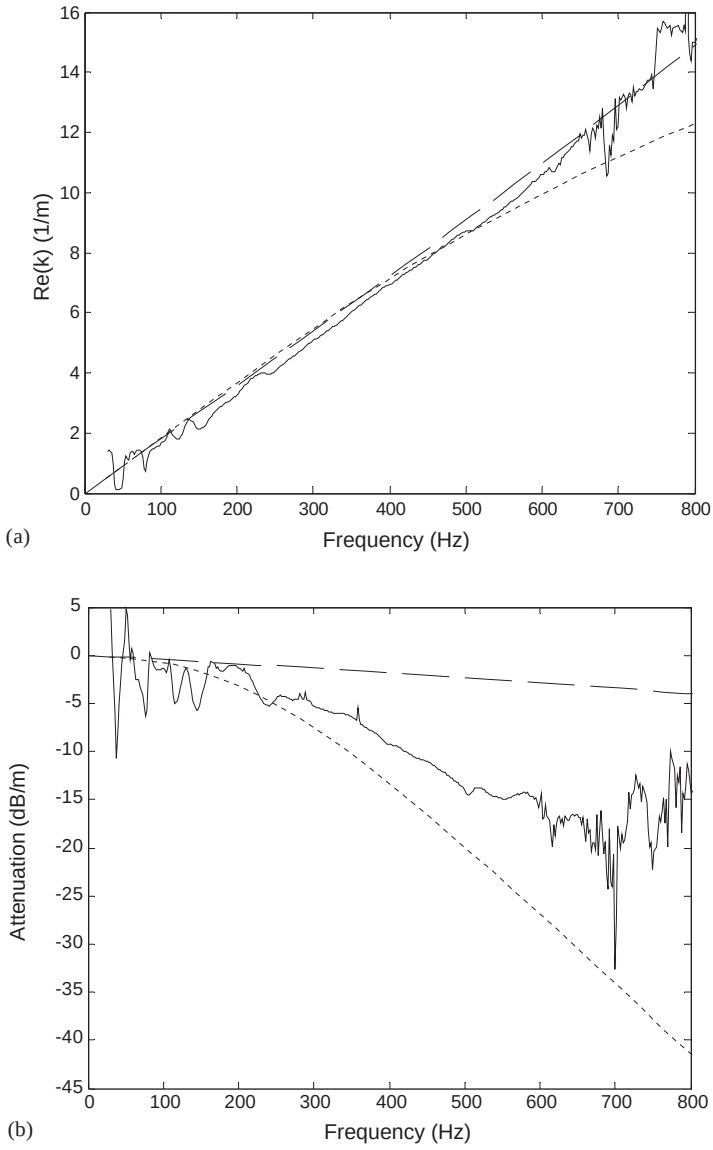

Fig. 4. Wavenumber for the axisymmetric 'fluid-borne' wave: (a) real part; (b) imaginary part. ——, measured; - - - -, predicted (buried pipe); – – –, predicted (in-vacuo pipe).

Table 2
Material properties of sandy soil

Density (kg/m^3)	1500
Longitudinal wavespeed (m/s)	200
Shear wavespeed (m/s)	100

minimally affected by the presence of the soil, the wave attenuation is markedly increased compared with the in-air case; furthermore, it is substantially greater than for the submerged pipe (Fig. 2c). The predicted component impedances, depicted in Fig. 5, show the positive radiation resistance dominating over the pipe wall impedance for most of the frequency range, and also that the mass loading effect here is small, explaining the little change in wavespeed.

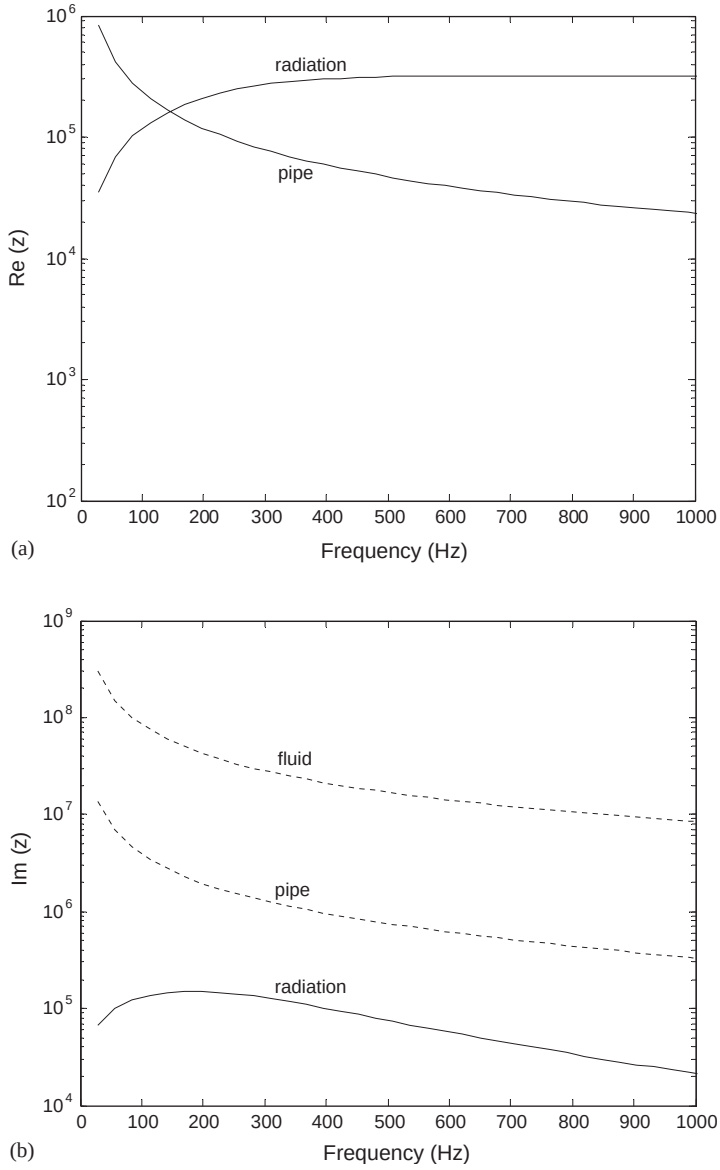

Fig. 5. Component impedances for buried pipe (predicted): (a) real part; (b) imaginary part. (dotted lines indicate negative values).

3.3. Discussion

The above results do not appear to explain the sudden disappearance of a leak noise signal when a water pipe becomes submerged, as the attenuation for a pipe buried in soil is somewhat greater than for the same pipe immersed in water. Furthermore, it is difficult to envisage a soil type in which the buried pipe wave attenuation would be lower than for the submerged pipe. However, in both cases, the attenuation is high. At low frequencies, the attenuation varies more or less linearly with frequency, so even at 100 Hz, the attenuation for the submerged pipe is of the order of 0.5 dB/m, indicating a halving of the wave energy in only 6 m, and in 12 m at 50 Hz. In soil with properties similar to that investigated here, the predicted attenuation is around 1 dB/m at 100 Hz, suggesting that any leak noise signal would not be detectable at any great distance regardless of whether the pipe became submerged at any point or not.

In many environments, the acoustic coupling between the pipe and the soil would not be as good as was the case for the sandy soil investigated here. If there were substantial air-pockets between the pipe and the ground, as might be the case if the soil was not as fine-grained, then the pipe/soil coupling could be severely compromised and the wave attenuation would be much closer to the in-air case. However, at low frequencies, the attenuation is almost identical under submerged in-air conditions, so even for a poorly coupled pipe, it is unlikely that the attenuation would increase as the pipe went from being buried in soil to being immersed in water.

Although not considered in the work described in this paper, it is likely that some acoustic energy is reflected at the soil/water interface as a result of the change in radiation conditions. However, preliminary analysis suggests that the transmission loss at this interface is not likely to be significant compared with the overall wave attenuation over distance.

4. Summary

In this paper, wavenumber measurements have been made on an in-air, and a submerged plastic water pipe. Excitation was applied directly in the fluid at frequencies well below the pipe ring frequency, so the dominant wavetype present was the axisymmetric ($n=0$), fluid-dominated ($s=1$) wave. Complex wavenumbers were determined, which encompass both the wavespeed and the wave attenuation. A three-transducer method was used to decompose the waves in the pipe, which was not terminated anechoically.

The measured wavenumbers were then compared with predictions from in-vacuo and submerged pipe models developed previously. In both cases, the wavespeed was found to compare well with that predicted by the model. The wavespeed for the in-vacuo pipe was found to be reduced substantially from the free-field value due to the pipe wall flexibility; when the pipe was submerged, this value was reduced yet further by the mass-loading of the pipe by the surrounding water. The measured attenuation was found to fluctuate, but the average values compared well with the predictions. For the submerged pipe, the model predicted an increase in the wave attenuation compared with the in-vacuo case, which was borne out in practice. However, the attenuation was found to be small compared with that for a pipe buried in sandy soil.

Unfortunately, the sudden disappearance of a leak noise signal when a water pipe becomes submerged cannot be easily explained; more on-site data are needed to determine the exact circumstances in which this phenomenon occurs before its origins could be more fully described.

Acknowledgements

The EPSRC are gratefully acknowledged for their support of this work.

References

[1] H.V. Fuchs, R. Riehle, Ten years of experience with leak detection by acoustic signal analysis, *Applied Acoustics* 33 (1991) 1–19.
[2] O. Hunaidi, W.T. Chu, Acoustical characteristics of leak signals in water distribution pipes, *Applied Acoustics* 58 (1999) 235–254.
[3] O. Hunaidi, W.T. Chu, A. Wang, W. Guan, Detecting leaks in plastic water distribution pipes, *Journal of the American Water Works Association* 92 (2000) 82–94.
[4] J.M. Muggleton, M.J. Brennan, R.J. Pinnington, Wavenumber prediction of waves in buried pipes for water leak detection, *Journal of Sound and Vibration* 249 (2002) 939–954.
[5] J.M. Muggleton, M.J. Brennan, P.W. Linford, Axisymmetric wave propagation in fluid-filled pipes: wavenumber measurements in in-vacuo and buried pipes, *Journal of Sound and Vibration* 270 (2004) 171–190.
[6] R.J. Pinnington, A.R. Briscoe, Externally applied sensor for axisymmetric waves in a fluid filled pipe, *Journal of Sound and Vibration* 173 (1994) 503–516.
[7] C.R. Fuller, F.J. Fahy, Characteristics of wave propagation and energy distributions in cylindrical elastic shells filled with fluid, *Journal of Sound and Vibration* 81 (1982) 501–518.
[8] D.I. Korteweg, Über die Fortpflanzungsgeschwindigkeit des Schalles in elastischen Röhren (On the speed of sound in water in flexible pipes), *Ann Physik* 5 (1878) 525–542.
[9] M.C. Junger, D. Feit, *Sound, Structures, and their Interaction*, MIT Press, Cambridge, MA, 1986.
[10] M.C. Junger, The physical interpretation of the expression for an outgoing wave in cylindrical coordinates, *The Journal of the Acoustical Society of America* 25 (1953) 40–47.
[11] J.M. Muggleton, M.J. Brennan, Axisymmetric wave propagation in buried, fluid-filled pipes: effects of the surrounding medium, in: *Proceedings of the IOA Spring Conference*, Salford, UK, 2002.